J|A|C|S
ARTICLES
Published on Web 08/29/2006

Homogeneously Alloyed CdS_xSe_{1-x} Nanocrystals: Synthesis, Characterization, and Composition/Size-Dependent Band Gap

Laura A. Swafford,[†] Lauren A. Weigand,[†] Michael J. Bowers II,[†] James R. McBride,[†] Jason L. Rapaport,[†] Tony L. Watt,[‡] Sriram K. Dixit,[‡] Leonard C. Feldman,[‡,§] and Sandra J. Rosenthal*[,†,‡,§]

Contributions from the Department of Chemistry, Vanderbilt University, 7330 Stevenson Center, Station B 351822, Nashville, Tennessee 37235-1822, Vanderbilt Interdisciplinary Program in Materials Science, 2301 Vanderbilt Place, VU Station B 350106, Nashville, Tennessee 37235-0106, and Department of Physics and Astronomy, Vanderbilt University, 6301 Stevenson Center, 1807 Station B, Nashville, Tennessee 37235-1807

Received June 14, 2006; E-mail: sandra.j.rosenthal@vanderbilt.edu

Abstract: Alloy nanocrystals provide an additional degree of freedom in selecting desirable properties for nanoscale engineering because their physical and optical properties depend on both size and composition. We report the pyrolytic synthesis of homogeneously alloyed CdS_xSe_{1-x} nanocrystals in all proportions. The nanocrystals are characterized using UV−visible absorption spectroscopy, transmission electron microscopy, X-ray diffractrometry, and Rutherford backscattering spectrometry to determine precisely structure, size, and composition. The dependence of band gap on nanocrystal size and composition is elucidated, yielding a bowing constant of 0.29, in agreement with bulk values. In addition, the morphology of the resultant nanocrystals can be altered by changing the reaction conditions, generating structures ranging from homogeneous, spherical nanocrystals to one-dimensional gradient nanorods.

Introduction

Semiconductor nanocrystals are of primary interest to several fields of research because of their unique optical properties. They exhibit quantum confinement effects such as size-dependent optical and electronic properties for applications in photovoltaics,[1−6] light-emitting diodes,[7−9] photocatalysis,[10−13] bioassays,[14−20] and electronics.[21−23] Specific applications, however, require multiple characteristics in a single system. For example, very small nanocrystals are desirable for in vivo imaging,[14] yet multiplexing experiments require a range of sizes in order to achieve a range of fluorescence colors. Size also plays a role when nanocrystals must be incorporated into larger superstructures such as mesoporous materials in photovoltaics.[4,24] One solution to the problem of dual requirements is to employ alloy nanocrystals. Since the optical properties of alloys vary with composition, it is possible to tune the spectrum while maintaining a small size. Thus, by varying composition, we gain a second tool for altering physical and optical properties. Both size and composition may be tuned to select multiple desirable qualities simultaneously.

To date, research into pseudobinary (AB_xC_{1-x}) semiconductor alloy nanocrystals has been limited.[25−33] In some cases, alloys

[†] Department of Chemistry, Vanderbilt University.
[‡] Vanderbilt Interdisciplinary Program in Materials Science.
[§] Department of Physics and Astronomy, Vanderbilt University.

(1) Swafford, L. A.; Rosenthal, S. J. In *Molecular Nanoelectronics*; Reed, E. M. A., Lee, T., Eds.; American Scientific Publishers: Stevenson Ranch, CA, 2003.
(2) Greenham, N. C.; Peng, X.; Alivisatos, A. P. *Phys. Rev. B* **1996**, *54*, 17628−17637.
(3) Huynh, W. U.; Dittmer, J. J.; Alivisatos, A. P. *Science* **2002**, *295*, 2425−2427.
(4) Robel, I.; Subramanian, V.; Kuno, M.; Kamat, P. V. *J. Am. Chem. Soc.* **2006**, *128*, 2385−2393.
(5) Schaller, R. D.; Klimov, V. I. *Phys. Rev. Lett.* **2004**, *92*, 186601.
(6) Mueller, A. H.; Petruska, M. A.; Achermann, M.; Werder, D. J.; Akhadov, E. A.; Koleske, D. D.; Hoffbauer, M. A.; Klimov, V. I. *Nano Lett.* **2005**, *5*, 1039−1044.
(7) Erwin, M. M.; Kadavanich, A. V.; McBride, J.; Kippeny, T.; Pennycook, S.; Rosenthal, S. J. *Eur. Phys. J. D* **2001**, *16*, 275−277.
(8) Bowers, M. J.; McBride, J. R.; Rosenthal, S. J. *J. Am. Chem. Soc.* **2005**, *127*, 15378−15379.
(9) Gao, M. Y.; Lesser, C.; Kirstein, S.; Mohwald, H.; Rogach, A. L.; Weller, H. *J. Appl. Phys.* **2000**, *87*, 2297−2302.
(10) Wang, L. G.; Pennycook, S. J.; Pantelides, S. T. *Phys. Rev. Lett.* **2002**, *89*, 075506.
(11) Henglein, A. *Pure Appl. Chem.* **1984**, *56*, 1215−1224.
(12) Henglein, A. *Ber. Bunsen-Ges. Phys. Chem. Chem. Phys.* **1997**, *101*, 1562−1572.
(13) Kho, R.; Nguyen, L.; Torres-Martinez, C. L.; Mehra, R. K. *Biochem. Biophys. Res. Commun.* **2000**, *272*, 29−35.
(14) Zimmer, J. P.; Kim, S. W.; Ohnishi, S.; Tanaka, E.; Frangioni, J. V.; Bawendi, M. G. *J. Am. Chem. Soc.* **2006**, *128*, 2526−2527.
(15) Bentzen, E. L.; House, F.; Utley, T. J.; Crowe, J. E.; Wright, D. W. *Nano Lett.* **2005**, *5*, 591−595.
(16) Dubertret, B.; Skourides, P.; Norris, D. J.; Noireaux, V.; Brivanlou, A. H.; Libchaber, A. *Science* **2002**, *298*, 1759−1762.
(17) Gerion, D.; Parak, W. J.; Williams, S. C.; Zanchet, D.; Micheel, C. M.; Alivisatos, A. P. *J. Am. Chem. Soc.* **2002**, *124*, 7070−7074.
(18) Rosenthal, S. J.; Tomlinson, I.; Adkins, E. M.; Schroeter, S.; Adams, S.; Swafford, L.; McBride, J.; Wang, Y. Q.; DeFelice, L. J.; Blakely, R. D. *J. Am. Chem. Soc.* **2002**, *124*, 4586−4594.
(19) Wu, X. Y.; Liu, H. J.; Liu, J. Q.; Haley, K. N.; Treadway, J. A.; Larson, J. P.; Ge, N. F.; Peale, F.; Bruchez, M. P. *Nat. Biotechnol.* **2003**, *21*, 41−46.
(20) Dahan, M.; Levi, S.; Luccardini, C.; Rostaing, P.; Riveau, B.; and Triller, A. *Science* **2003**, *302*, 442−445.
(21) Klein, D. L.; Roth, R.; Lim, A. K. L.; Alivisatos, A. P.; McEuen, P. L. *Nature* **1997**, *389*, 699−701.
(22) Konenkamp, R.; Hoyer, P.; Wahi, A. *J. Appl. Phys.* **1996**, *79*, 7029−7035.
(23) Vlasov, Y. A.; Yao, N.; Norris, D. J. *Adv. Mater.* **1999**, *11*, 165−169.
(24) Peter, L. M.; Riley, D. J.; Tull, E. J.; Wijayantha, K. G. U. *Chem. Commun.* **2002**, 1030−1031.

have been the unintentional result of an attempt to synthesize a different crystal structure.[25,26] They have also been successfully employed as shell materials for binary nanocrystals;[26−28] a shell that combines the core semiconductor with a higher-band-gap semiconductor generates increased fluorescence due to confinement of the electron and hole to the core while simultaneously ameliorating undesirable interface effects, such as lattice mismatch leading to incomplete shell growth.[26] A number of studies have examined the optical properties of alloy nanocrystals, but either the alloys are shown to have a gradient structure,[25,29] in which the composition of the alloy is different in different parts of the nanocrystal, or no analysis into the homogeneity of the alloy is provided.[30,31] The distinction between a gradient alloy and a homogeneous one is critical because, as we and others show, gradient alloy nanocrystals show optical properties that are significantly different than homogeneous alloys.[32] Kuno and co-workers' study of $HgSe_{1-x}S_x$ nanocrystals presents a highly detailed examination of the optical properties of homogeneous nanocrystals, but for a single size.[33] To our knowledge, only Bailey and Nie's study of $CdSe_xTe_{1-x}$ nanocrystals has explored the effect of alloy composition on the optical properties of homogeneous nanocrystals of several different sizes.[32]

Much of the difficulty in alloy nanocrystal research lies in devising a synthetic scheme to produce the desired alloy structure, be it homogeneous or gradient. To achieve homogeneous alloys, the growth rates of the two constituent materials must be equal[29,32] and the conditions necessary for the growth of one constituent cannot impede the growth of the other. In addition, the structure and bonding of the two materials must be sufficiently similar to allow their facile mixing, otherwise the formation of segregated structures such as core/shells or two different binary nanocrystals may result. In this work, we report the synthesis of homogeneous CdS_xSe_{1-x} nanocrystals over the range $x = 0-1$ using a single synthetic method. The nanocrystals are characterized with respect to structure, composition, size, and optical band gap, and on the basis of these, the dependence of band gap on size and composition is extracted. In addition, by varying the concentration of one of the ligands in the synthesis, we show that we can alter the morphology of the nanocrystals from homogeneous nanocrystals to highly fluorescent, gradient nanocrystals to nanorods with a strong gradient occurring in a single direction, which could be very useful for unidirectional charge transport in nanoelectronic devices.

Experimental Section

Materials. Cadmium oxide (CdO, 99.99%), oleic acid (OA, 90%), tri-*n*-butylphosphine (TBP, 93%), and octadecene (ODE, 90%) were purchased from Aldrich. Selenium shot (Se, 99.99%) was purchased from Strem. Sulfur powder (S, USP sublimed) was purchased from Fisher Scientific. A concentrated selenium stock solution (4 M) was prepared by dissolving 0.79 g of Se in 2.5 mL of TBP and sonicating to achieve complete dissolution. This solution was either used as prepared in growth solutions for larger nanocrystals or was diluted to 100 mL in ODE to produce a 0.1 M Se stock solution. A sulfur stock solution (0.1 M) was prepared by adding 0.32 g of S to 100 mL of ODE and heating to 50−100 °C for several hours until all sulfur had dissolved.

Nanocrystal Synthesis. The synthesis of the alloy nanocrystals was based on the syntheses of CdS and CdSe by Yu and Peng.[34] Typically, 256 mg of CdO, 2.4 mL of OA, and 10 mL of ODE were heated to 315 °C in a 100 mL three-neck round-bottom flask under argon. At 275−280 °C, the solution turned colorless, indicating the formation of cadmium oleate. To produce nanocrystals of composition CdS_xSe_{1-x}, a solution composed of $10x$ mL of S stock solution and $10(1 - x)$ mL of 0.1 M Se stock solution was swiftly injected into the flask via a large-bore needle once it had reached 315 °C. The temperature was then lowered to 275 °C, and the nanocrystals were allowed to grow until the desired size had been achieved (<15 min).

For nanocrystals larger than ∼40 Å, addition of a growth solution was required. 0.76 g of CdO, 6 mL of OA, and 25 mL of ODE were heated to 290 °C under argon until the solution turned colorless. The solution was then cooled to 50−100 °C, and $0.16x$ g of S powder was added, stirring until dissolved. Finally, the solution was removed from heat, and $1.25(1 - x)$ mL of 4 M Se stock solution was added once the Cd/S solution had cooled to 30 °C. This growth solution was added dropwise to the nanocrystal reaction vessel at the rate of 3 mL/min, beginning just after the initial S/Se injection. It is noted that this reaction can be scaled up.

Once synthesized, the nanocrystals were isolated by precipitation with a mixture of butanol and ethanol, then centrifuged, and the resulting nanocrystal pellet was resuspended in a small amount of hexane (∼3 mL). We found that ODE and excess OA adhered strongly to the nanocrystals, so samples were washed eight times prior to characterization. Rutherford backscattering spectrometry of the waste from the washes confirmed that this amount of washing was sufficient to remove any remaining precursor material; in addition, with eight washes, we observed no contamination from excess organic molecules in the Rutherford backscattering and transmission electron microscopy data.

Characterization. UV−visible absorption spectra were obtained with a Varian Cary 50 UV−vis spectrophotometer. Clean nanocrystals were suspended in hexanes and diluted to an optical density of 0.6−0.8 at the lowest energy peak. The optical band gap was taken as the wavelength at the maximum of this peak. Photoluminescence (PL) and photoluminescent excitation (PLE) spectra were taken on an ISS PC1 photon counting spectrofluorometer. Sample preparation for PL and PLE spectra was identical to that for absorption spectra. High-resolution transmission electron microscopy (TEM) images were taken on a Phillips CM20 200 kV TEM. Samples were prepared by placing a drop of nanocrystals diluted in hexanes to an optical density of <0.1 onto an ultrathin carbon-on-Formvar TEM grid (Ted Pella, Inc.), wicking away any excess solvent. Images were obtained at a calibrated magnification of 420 k×. To determine the average diameter of a sample of nanocrystals, 200−300 of the imaged nanocrystals were measured along the C_3 axis. X-ray diffraction (XRD) scans were obtained using a Scintag X_1 $\theta/2\theta$ automated powder X-ray diffractometer with a Cu target ($\lambda = 1.54056$ Å), a Peltier-cooled solid-state detector, and a zero-background, Si(510) sample support. Rutherford backscattering spectrometry (RBS) was performed using a custom-built setup.[35] Samples were prepared by coating the surface of a pyrolytic graphite substrate (Carbone of America) with nanocrystals diluted in hexanes to an optical density of 0.4−0.6, wicking to remove excess solvent. Experiments were performed in a high vacuum chamber (<10^{-6}

(25) Qian, H. F.; Qiu, X.; Li, L.; Ren, J. C. *J. Phys. Chem. B* **2006**, *110*, 9034−9040.
(26) McBride, J.; Treadway, J.; Feldman, L. C.; Pennycook, S. J.; Rosenthal, S. J. *Nano Lett.* **2006**, *6*, 1496−1501.
(27) Qian, H. F.; Li, L.; Ren, J. C. *Mater. Res. Bull.* **2005**, *40*, 1726−1736.
(28) Zhong, X. H.; Han, M. Y.; Dong, Z. L.; White, T. J.; Knoll, W. *J. Am. Chem. Soc.* **2003**, *125*, 8589−8594.
(29) Jang, E.; Jun, S.; Pu, L. *Chem. Commun.* **2003**, 2964−2965.
(30) Zhong, X. H.; Feng, Y. Y.; Knoll, W.; Han, M. Y. *J. Am. Chem. Soc.* **2003**, *125*, 13559−13563.
(31) Tian, Y. C.; Newton, T.; Kotov, N. A.; Guldi, D. M.; Fendler, J. H. *J. Phys. Chem.* **1996**, *100*, 8927−8939.
(32) Bailey, R. E.; Nie, S. M. *J. Am. Chem. Soc.* **2003**, *125*, 7100−7106.
(33) Kuno, M.; Higginson, K. A.; Qadri, S. B.; Yousuf, M.; Lee, S. H.; Davis, B. L.; Mattoussi, H. *J. Phys. Chem. B* **2003**, *107*, 5758−5767.
(34) Yu, W. W.; Peng, X. G. *Angew. Chem., Int. Ed.* **2002**, *41*, 2368−2371.
(35) Taylor, J.; Kippeny, T.; Rosenthal, S. J. *J. Cluster Sci.* **2001**, *12*, 571−582.

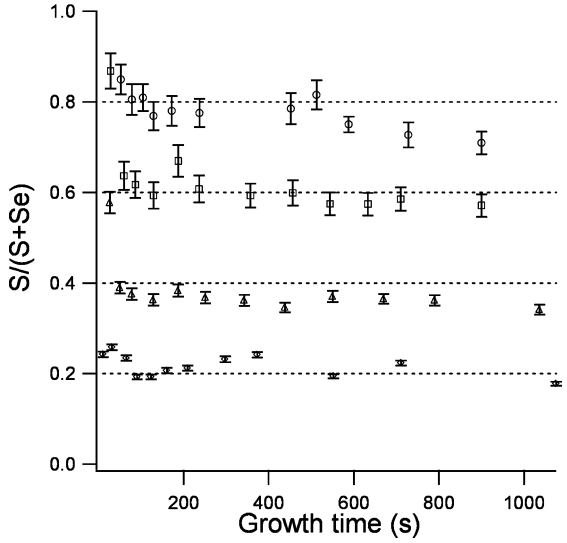

Figure 1. Alloy composition as a function of growth time for $CdS_{0.8}Se_{0.2}$ (○), $CdS_{0.6}Se_{0.4}$ (□), $CdS_{0.4}Se_{0.6}$ (Δ), and $CdS_{0.2}Se_{0.8}$ (◊). RBS analysis of aliquots of nanocrystals pulled from single batches of nanocrystals during growth reveals that the composition of the nanocrystals remains reasonably constant over the growth period, an indication of alloy homogeneity.

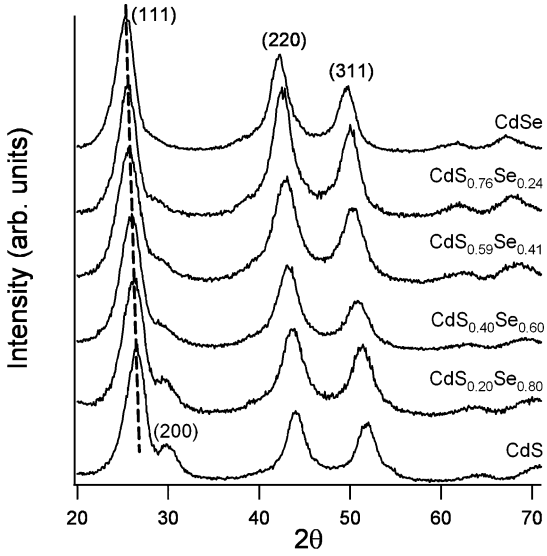

Figure 2. XRD spectra of CdS_xSe_{1-x} nanocrystals. Spectra have been normalized to the height of the (111) peak and offset vertically. The spectra characterize a zinc-blende structure,[42,43] with a linear change in lattice spacing from $x = 0$ to 1 (e.g., see dashed line) and a gradual subsidence of the (200) peak, indicating the formation of alloy nanocrystals rather than a mixture of CdS and CdSe particles.

Torr) with a 1.8 MeV ^{4}He ion beam at normal incidence. Backscattered ions were collected at an angle of 176° with a solid-state detector. Spectra were analyzed according to Feldman et al.,[36] yielding the elemental composition of the nanocrystals.

Results and Discussion

Homogeneity and Structure. In order to confirm that the nanocrystals were indeed homogeneous, batches of nanocrystals were grown to large size, with the periodic removal of aliquots of the growing nanocrystals. The aliquots were then washed and analyzed by RBS to determine composition. As demonstrated in Figure 1, except very early in nanocrystal growth, the composition remained nearly constant over the growth period, indicating that the alloys were homogeneous, rather than gradient or core/shell in nature. It should be noted that at the very smallest sizes, all nanocrystals were shown to be sulfur-rich by RBS. There are two possible explanations for this observation. The first is simply that it is very difficult to clean the smallest nanocrystals, so RBS may be detecting unreacted sulfur precursor. The second explanation is that the kinetics of nucleation are different than the kinetics of growth, resulting in sulfur enrichment at the smallest sizes. Indeed, the smallest sizes are most likely magic-number nanocrystals, composed of only a few atoms.[8,37−41] CdSe nanocrystals halted at the same stage of growth displayed the same absorption and emission characteristics as magic-number nanocrystals produced previously by a different synthesis.[8] If it is true that the nucleation kinetics in this reaction favor the formation of sulfur-rich seeds, these seeds are very small. As seen in Figure 1, the nanocrystals achieve the expected composition within 30 s, suggesting that the sulfur-rich seeds are so small that they constitute a nearly negligible portion of larger nanocrystals. As we shall see later, the sulfur-rich seeds do not seem to affect the dependence of band gap on size and composition; therefore, we consider the nanocrystals larger than the seeds to be essentially homogeneous.

This conclusion is supported by XRD spectra of the nanocrystals (Figure 2), which show a linear change in lattice spacing as composition changes from CdS to CdSe (e.g., dashed line). If the nanocrystals were a mixture of CdS nanocrystals and CdSe nanocrystals instead of alloys, the resultant XRD spectra would exhibit a superposition of the spectra of pure CdS and pure CdSe. It is noted that core/shell nanocrystals also show spectra that are intermediate between the spectra of the core and the shell.[44,45] However, since the RBS data show little change in composition with size, core/shell structures are unlikely; to maintain a core/shell structure throughout nanocrystal growth would necessitate constant rearrangement of interior atoms, which is highly unlikely. The spectra also show a zinc-blende conformation throughout the range of compositions, in contrast to Yu and Peng's synthesis,[34] which shows a mix of zinc-blende and wurtzite structures. The zinc-blende structure is likely due to the surfactant system used;[43,46,47] that there are fewer wurtzite stacking faults may reflect the higher temperatures at which the synthesis was conducted or the lower amount of tributylphosphine used (1:1 Se/TBP molar ratio).

High-resolution TEM images confirm the zinc-blende structure and appear spherical with a few aberrant pyramids (Figure 3). An indication of the narrow size distribution is that these nanocrystals readily form arrays on the carbon film support.[48]

(36) Feldman, L. C.; Mayer, J. W. *Fundamentals of Surface and Thin Film Analysis*; North Holland-Elsevier: New York, 1986.
(37) Peng, Z. A.; Peng, X. G. *J. Am. Chem. Soc.* **2002**, *124*, 3343−3353.
(38) Qu, L.; Yu, W. W.; Peng, X. G. *Nano Lett.* **2004**, *4*, 465−469.
(39) Landes, C.; Braun, M.; Burda, C.; El-Sayed, M. A. *Nano Lett.* **2001**, *1*, 667−670.
(40) Landes, C.; El-Sayed, M. A. *J. Phys. Chem. A* **2002**, *106*, 7621−7627.
(41) Chen, X. B.; Samia, A. C. S.; Lou, Y. B.; Burda, C. *J. Am. Chem. Soc.* **2005**, *127*, 4372−4375.
(42) Urbieta, A.; Fernández, P.; Piqueras, J. *J. Appl. Phys.* **2004**, *96*, 2210−2213.
(43) Mohamed, M. B.; Tonti, D.; Al-Salman, A.; Chemseddine, A.; Chergui, M. *J. Phys. Chem. B* **2005**, *109*, 10533−10537.
(44) Li, J. J.; Wang, Y. A.; Guo, W. Z.; Keay, J. C.; Mishima, T. D.; Johnson, M. B.; Peng, X. G. *J. Am. Chem. Soc.* **2003**, *125*, 12567−12575.
(45) Peng, X. G.; Schlamp, M. C.; Kadavanich, A. V.; Alivisatos, A. P. *J. Am. Chem. Soc.* **1997**, *119*, 7019−7029.
(46) Jasieniak, J.; Bullen, C.; van Embden, J.; Mulvaney, P. *J. Phys. Chem. B* **2005**, *109*, 20665−20668.
(47) Yu, W. W.; Wang, Y. A.; Peng, X. G. *Chem. Mater.* **2003**, *15*, 4300−4308.

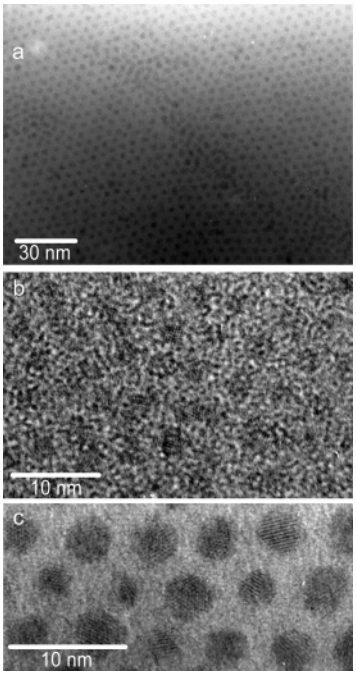

Figure 3. TEM images of $CdS_{0.8}Se_{0.2}$ (a), $CdS_{0.4}Se_{0.6}$ (b), and $CdS_{0.2}Se_{0.8}$ (c) show a highly crystalline, spherical, primarily zinc-blende structure with a few wurtzite stacking faults. Size dispersity is low, allowing the nanocrystals to array on the TEM grid.

The average size distribution of the samples was measured using TEM images was 11.5% (standard deviation); this number is likely slightly larger than the true distribution due to the method of measuring.

Optical Properties and Bowing Constant. Figure 4a shows typical UV−vis absorption and PL spectra for the alloy nanocrystals. The spectra appear similar to those of CdS and CdSe nanocrystals. Absorption spectra are characterized by several distinct peaks, an indication of good size distribution. The spacing and intensity of these peaks show some variation (e.g., see Figure 5b), indicating potentially intriguing electronic structure in the alloys. The PLE spectra of the nanocrystals confirm that the cause is not inhomogeneity in the samples (e.g., Figure 4b). PL spectra are characterized by two peaks: a higher-energy, narrow (30−38 nm fwhm) peak assigned to band edge emission and a lower-energy, broad peak assigned to "deep trap" emission, caused by trapping of the photoexcited hole to unpassivated surface anion orbitals.[49−51] The band edge emission is red-shifted from the band edge absorption peak by 5−30 nm, with smaller nanocrystals showing larger shifts. Likewise, the relative intensity of deep trap emission varies from none in large nanocrystals to a peak intensity on the order of the intensity of the band edge emission for small nanocrystals; this behavior is similar to CdSe nanocrystals synthesized in tri-*n*-octylphosphine oxide (TOPO).[49]

The behavior of alloys is characterized by Végard's Law, which states that, while lattice constant changes linearly with composition, as seen in Figure 2, other physical properties such

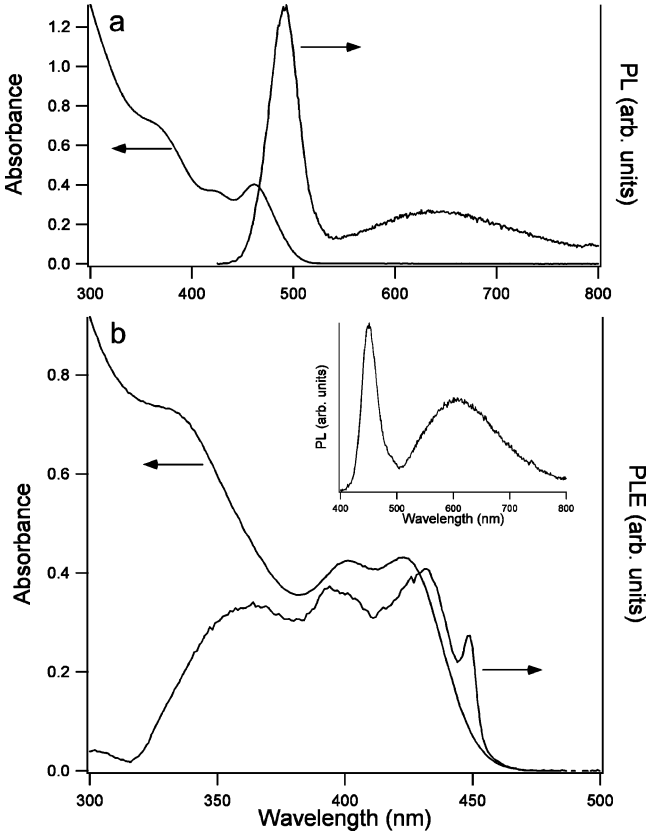

Figure 4. (a) Absorbance and PL spectra of 35 Å $CdS_{0.53}Se_{0.47}$ nanocrystals. These spectra typify the optical properties of the alloy nanocrystals. (b) Absorbance and PLE spectra of 24 Å $CdS_{0.70}Se_{0.30}$ nanocrystals. The PLE spectrum, taken at the maximum of the band edge emission (450 nm), agrees closely with the absorption spectrum close to the band edge, an indication that the sample is homogeneous. The inset shows the PL spectrum for this sample. The PL spectra in (a) and (b) were taken with an excitation wavelength of 367 nm.

as band gap often vary nonlinearly.[52] To first approximation, the variation is quadratic:

$$E_g(CdS_xSe_{1-x}) = xE_g(CdS) + (1-x)E_g(CdSe) - bx(1-x) \quad (1)$$

where the bowing constant, *b*, describes the extent of nonlinearity. The sources of nonlinearity are threefold: (i) the changing lattice constant alters the band structure; (ii) the atoms in the alloy have different electronegativities, deforming the electron distribution; and (iii) anion−cation bond lengths and angles must relax in order to accommodate the differently sized constituents.[53,54] In the case of nanocrystals of *any* composition, quantum confinement also dictates a size dependence:[55]

$$E_g(d) = E_g(\infty) + \frac{a}{d} + \frac{c}{d^2} \quad (2)$$

where *d* is the nanocrystal diameter and *a* and *c* are empirical fit parameters.[56] The dependence of band gap on size and on composition are demonstrated in Figure 5. Substituting eq 2

(48) Murray, C. B.; Kagan, C. R.; Bawendi, M. G. *Annu. Rev. Mater. Sci.* **2000**, *30*, 545−610.
(49) Underwood, D. F.; Kippeny, T.; Rosenthal, S. J. *J. Phys. Chem. B* **2001**, *105*, 436−443.
(50) Katari, J. E. B.; Colvin, V. L.; Alivisatos, A. P. *J. Phys. Chem.* **1994**, *98*, 4109−4117.
(51) Shiang, J. J.; Kadavanich, A. V.; Grubbs, R. K.; Alivisatos, A. P. *J. Phys. Chem.* **1995**, *99*, 17417−17422.
(52) Végard, L. *Z. Phys.* **1921**, *5*, 17−26.
(53) Bernard, J. E.; Zunger, A. *Phys. Rev. B* **1987**, *36*, 3199−3228.
(54) Böer, K. W. *Survey of Semiconductor Physics: Electrons and Other Particles in Bulk Semiconductors*; Van Nostrand Reinhold: New York, 1990.
(55) Brus, L. E. *J. Chem. Phys.* **1984**, *80*, 4403−4409.

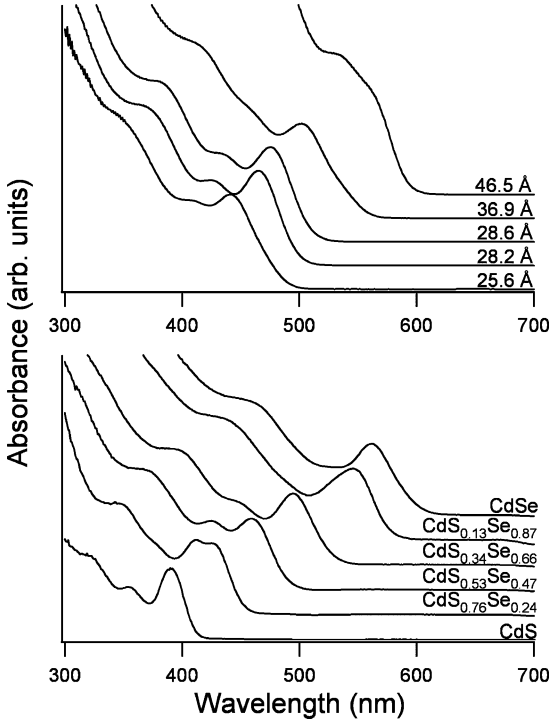

Figure 5. Linear UV−visible absorption spectra demonstrating dependence of band gap on size and composition: (top) size dependence of ~$CdS_{0.4}Se_{0.6}$ nanocrystals; (bottom) composition dependence of ~30 Å nanocrystals.

into eq 1, we find that the dependence of band gap on size and composition is given by

$$E_g(x,d) = x\left[E_g(\mathrm{CdS},\infty) + \frac{a_1}{d} + \frac{c_1}{d^2}\right] + (1-x)\left[E_g(\mathrm{CdSe},\infty) + \frac{a_2}{d} + \frac{c_2}{d^2}\right] - b(d)x(1-x) \quad (3)$$

In this expression, the bowing constant is expressed as a function of the nanocrystal diameter. The size dependence is included for a number of reasons. First, lattice spacing is known to decrease slightly with decreasing nanocrystal diameter, a function of surface tension.[58] Second, surface reconstruction can affect cation−anion bond lengths, as well as electron distribution.[59−61] Third, ligand effects can also alter cation−anion bond lengths and charge distribution.[60] Combined, these effects could significantly impact the bowing constant, particularly at small diameters. It is noted that, in eq 3, any nonlinearity in the change in the parameters *a* and *c* between their CdS and CdSe values is contained within the bowing constant; if these values vary with composition in a manner different than the bulk band gap (E_g(CdS,∞) and E_g(CdSe,∞)), then the bowing constant should depend on size.

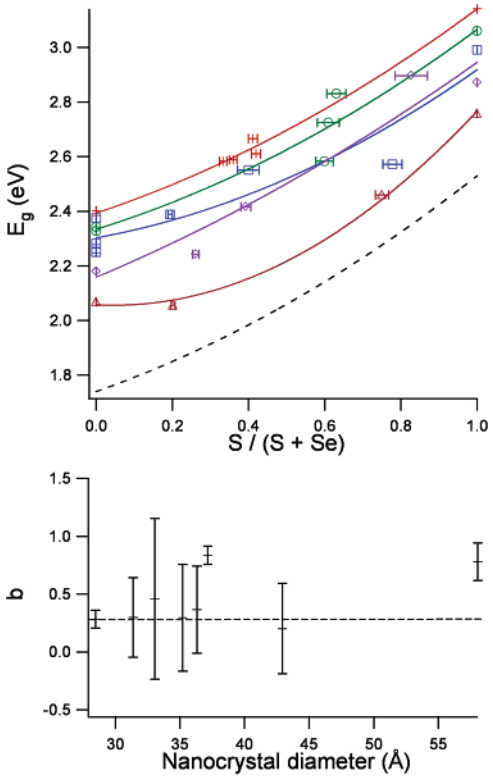

Figure 6. Bowing vs size for CdS_xSe_{1-x} nanocrystals. (top) Band gap as a function of composition for 28 (+), 31 (○), 36 (□), 43 (◊), and 58 Å (Δ) nanocrystals. Curves show the bowing, which remains relatively constant and closely follows the bulk bowing behavior (dashed line from eq 1; E_g(CdS,∞) = 2.53 eV,[64] E_g(CdSe,∞) = 1.74 eV,[64] b = 0.3[58,65,66]). Values for CdS and CdSe nanocrystals were either measured in this work, extrapolated from Yu et al.,[60] or calculated from a fit to the data of Yu et al. (Table 1). For clarity, only five sizes are shown. (bottom) Bowing constant as a function of nanocrystal diameter. The dashed line indicates the bowing constant, 0.29, obtained by fitting all data to eq 3. From this graph, it is evident that the bowing constant remains constant (within the uncertainty of the data) over the range of the experiment.

Figure 6 shows the dependence of bowing constant on size. Results show that, within the uncertainty and range of this work, the bowing constant is in fact insensitive to diameter, in agreement with previous work on $CdSe_xTe_{1-x}$.[32] This suggests that the small change in lattice constant with size is not enough to significantly impact the band structure. More intriguingly, it suggests that the surface and surrounding environment (ligands and solvent), which are known to impact strongly the optical and electronic behavior of nanocrystals,[55,62−67] do not affect nanocrystal band gap bowing beyond their effects on the size dependence of the band gap. As size decreases and the surface-to-volume ratio increases, surface effects play an increasingly important role in nanocrystal behavior, distorting bonding, and electronic structure, which might affect bowing for the reasons mentioned above. Finally, the fact that the bowing in these nanocrystals is identical to bulk values suggests that any structural anomalies and compositional fluctuations, both of

(56) In Brus' original work,[55] the parameters *a* and *c* have physical meaning based on bulk material properties such as effective mass and dielectric constant; however, due to the failure of the effective mass approximation at small diameters,[55, 57] we have found that a much better fit is attained when *a* and *c* are allowed to float.

(57) Kippeny, T.; Swafford, L. A.; Rosenthal, S. J. *J. Chem. Ed.* **2002**, *79*, 1094−1100.
(58) Tolbert, S. H.; Alivisatos, A. P. *J. Chem. Phys.* **1995**, *102*, 4642−4656.
(59) Bawendi, M. G.; Kortan, A. R.; Steigerwald, M. L.; Brus, L. E. *J. Chem. Phys.* **1989**, *91*, 7282−7290.
(60) McGinley, C.; Riedler, M.; Moller, T.; Borchert, H.; Haubold, S.; Haase, M.; Weller, H. *Phys. Rev. B* **2002**, *65*, 245308.
(61) Rabani, E. *J. Chem. Phys.* **2001**, *115*, 1493−1497.
(62) Wang, L. W.; Zunger, A. *Phys. Rev. B* **1996**, *53*, 9579−9582.
(63) Guyot-Sionnest, P.; Wehrenberg, B.; Yu, D. *J. Chem. Phys.* **2005**, *123*, 074709.
(64) Kalyuzhny, G.; Murray, R. W. *J. Phys. Chem. B* **2005**, *109*, 7012−7021.
(65) Myung, N.; Bae, Y.; Bard, A. J. *Nano Lett.* **2003**, *3*, 747−749.
(66) Califano, M.; Franceschetti, A.; Zunger, A. *Nano Lett.* **2005**, *5*, 2360−2364.
(67) Kippeny, T. C.; Bowers, M. J., II; McBride, J. R.; Rosenthal, S. J. Submitted for publication.

Table 1. Fitting Parameters for Calculation of Bowing Constant

	a_{CdS} (eV–Å)	c_{CdS} (eV–Å²)	a_{CdSe} (eV–Å)	c_{CdSe} (eV–Å²)	B
fixed[a]	8.4 ± 2.1	245 ± 34	19.6 ± 0.8	−28.8 ± 7.5	0.31 ± 0.10
floated[b]	7.9 ± 2.7	252 ± 44	19.5 ± 0.8	−28.0 ± 7.0	0.29 ± 0.16

[a] a and c were calculated by fitting CdS and CdSe data from Yu et al.,[70] as well as our data to eq 2, with $E_g(\infty)$ fixed at 2.53[74] and 1.74 eV,[74] respectively. These values were then substituted into eq 3 to obtain the bowing constant. [b] The bulk band gaps of 2.53[74] and 1.74 eV[74] for CdS and CdSe, respectively, were substituted into eq 3 to obtain the bowing constant, as well as a and c.

which are known to contribute to the bowing phenomenon,[53,68,69] are not severe enough to affect the optoelectronic behavior of the nanocrystals, so that they can indeed be considered homogeneous.

With this information, the band gaps, compositions, and diameters of 36 alloy samples ranging in diameter from 20 to 80 Å were combined with band gap and size data for CdS and CdSe from Yu et al.[70] and fit to eq 3 in two ways, summarized in Table 1. First, all data for CdS and CdSe were fit to eq 2 to obtain a and c for the two materials.[71] These values for a and c were then substituted into eq 3 along with the bulk band gaps, yielding a bowing constant of 0.31 ± 0.10. Next, the fit was repeated, but a and c were allowed to float, yielding a bowing constant of 0.29 ± 0.16. These values are in good agreement; moreover, they agree well with the bulk bowing constant, which has been reported as 0.3[68,75,76] or less than 0,[69,77,78] presumably due to differences in synthetic and analytical techniques; others have suggested that the work showing negative bowing constants was performed on thin films whose actual composition and homogeneity may be suspect.[75] In addition, the values for a and c obtained from eq 3 when they were allowed to float agree well with their values from fits to pure CdS and CdSe.

That the observed bowing constant in the nanocrystals agrees with the bulk value and that the bowing constant, a, and c were approximately identical regardless of how the data were fit suggests that a and c are linear combinations of the binary constituents. Consequently, we may simplify eq 3 to

$$E_g(x,d) = E_g(x,\infty) + \frac{a_x}{d} + \frac{c_x}{d^2} \tag{4}$$

where $E_g(x,\infty)$ is given by eq 1 and a_x and c_x are the linear combinations

$$a_x = xa_1 + (1-x)a_2$$
$$c_x = xc_1 + (1-x)c_2 \tag{5}$$

Equation 4 is a more elegant form of eq 3 because it shows the traditional dependence of band gap on size for nanocrystals (e.g., eq 2); moreover, it demonstrates that the bowing constant is independent of both size and the empirical parameters, a and c.

Regardless of the degree of bowing, these results demonstrate that, by varying the composition of the nanocrystals, we have introduced an additional means of tuning their properties. Multiple wavelengths can be generated by a single size, which could be useful when size requirements are specific, such as in biological imaging, where small nanocrystals are desirable. In addition, by using alloys, we can easily achieve band gaps (and other properties) which otherwise would be difficult to achieve. For example, in the case of CdS and CdSe, making nanocrystals with a band gap of 2.6 eV (480 nm) is normally difficult; CdS nanocrystals would need to be very large (>100 Å), often resulting in a large size dispersity, while CdSe nanocrystals would conversely be very small (21 Å), difficult to synthesize accurately due to the speed of most reactions, difficult to image by TEM, and less stable than medium and large nanocrystals. $CdS_{0.8}Se_{0.2}$, however, produces the same band gap with a nanocrystal diameter of 32 Å, which is an ideal size from the standpoint of synthesis, imaging, and stability. We anticipate that for these and other reasons, alloys will play an increasingly important role in nanoengineering.

Growth Kinetics and Effect of TBP. In order to synthesize homogeneous CdS_xSe_{1-x} nanocrystals, sulfur and selenium must be added at the same rate to the growing nanocrystals. While the exact mechanisms of nanocrystal nucleation and growth are not known,[37,79−81] and the kinetics are debated,[34,80] it is reasonable to assume that the reactivities of cadmium monomer toward the two anions on the nanocrystal surface should not be markedly different, given that sulfur and selenium are isoelectronic and have very similar Lewis basicities. If the reactivities were very different, it is likely that a homogeneous alloy would be difficult if not impossible to achieve. Assuming that the rate of addition of cadmium to the growing nanocrystal is largely independent of the anion species to which it binds, and assuming that the rates of addition of sulfur and selenium obey first-order kinetics with respect to anion concentration, then the ratio of these rates is proportional to the ratio of the concentrations of sulfur and selenium:

$$\frac{\frac{d[\text{AS-S}]}{dt}}{\frac{d[\text{AS-Se}]}{dt}} = \frac{k_1[\text{AS}][\text{S}]}{k_2[\text{AS}][\text{Se}]} = \frac{k_1}{k_2}\frac{[\text{S}]}{[\text{Se}]} \tag{6}$$

Here AS is an available site for anion bonding and k_1 and k_2 are rate constants. This model of growth kinetics suggests two means of balancing these rates. For the rates to remain identical throughout nanocrystal growth, either the concentrations of sulfur and selenium must not change significantly during growth or k_1 and k_2 must be identical.

(68) Naumov, A.; Permogorov, S.; Reznitsky, A.; Verbin, S.; Klochikhin, A. *J. Cryst. Growth* **1990**, *101*, 713−717.
(69) Kumar, V.; Sharma, T. P. *J. Phys. Chem. Solids* **1998**, *59*, 1321−1325.
(70) Yu, W. W.; Qu, L. H.; Guo, W. Z.; Peng, X. G. *Chem. Mater.* **2003**, *15*, 2854−2860.
(71) No distinction was made between wurtzite and zinc-blende nanocrystals in the case of CdS and CdSe; because of the negligible differences in band gap and lattice constant for the bulk materials in the two conformations,[72−74] it was assumed that the size dependence of the band gap was likewise similar.
(72) Trindade, T.; O' Brien, P.; Pickett, N. L. *Chem. Mater.* **2001**, *13*, 3843−3858.
(73) Kadavanich, A. V. The Structure and Morphology of Semiconductor Nanocrystals. Ph.D. Thesis, Chemistry Department, University of California, Berkeley, 1997.
(74) Landolt, H. *Landolt-Börnstein: Numerical Data and Functional Relationships in Science and Technology*; Madelung, O., Ed.; Springer: New York, 1982; Vol. III-17b.
(75) Wei, S.-H.; Zhang, Z. B.; Zunger, A. *J. Appl. Phys.* **2000**, *87*, 1304−1311.
(76) Goede, O.; Hennig, D.; John, L. *Phys. Status Solidi B* **1979**, *96*, 671−681.
(77) Mane, R. S.; Lokhande, C. D. *Thin Solid Films* **1997**, *304*, 56−60.
(78) Kainthla, R. C.; Pandya, D. K.; Chopra, K. L. *J. Electrochem. Soc.* **1982**, *129*, 99−102.
(79) Peng, Z. A.; Peng, X. G. *J. Am. Chem. Soc.* **2001**, *123*, 1389−1395.
(80) Bullen, C. R.; Mulvaney, P. *Nano Lett.* **2004**, *4*, 2303−2307.
(81) Peng, Z. A.; Peng, X. G. *J. Am. Chem. Soc.* **2001**, *123*, 183−184.

The first approach was used successfully by Bailey and Nie[32] in the synthesis of $CdSe_xTe_{1-x}$ nanocrystals. By employing a cadmium-limited reaction, in which there was a large excess of anion precursor relative to cadmium, they limited the number of sites available for anion binding to the extent that selenium and tellurium concentrations remained essentially constant throughout the reaction, so the rate constants were immaterial. Indeed, when they increased the amount of cadmium, they grew gradient alloys because the rate constants were unequal. In initial attempts to produce homogeneous CdS_xSe_{1-x}, two different synthetic schemes were applied—a dimethylcadmium-based synthesis devised by Kippeny et al.[67] and the cadmium oxide synthesis presented here in the experimental section. Unfortunately, neither synthesis was successfully adapted to produce high-quality nanocrystals under cadmium-limited conditions. These results are in agreement with other research showing that cadmium oxide must be kept in excess of anion concentration.[80,81]

The second approach to equalizing the reaction rates of sulfur and selenium was the equalization of the rate constants or the tuning of the reactivities of the anion precursors. Studies have shown that the rate of nanocrystal growth is sensitive not only to precursor species but to ligand concentrations as well.[34,47,80,81] Fortunately, in the synthesis presented in the Experimental Section, a means of tuning the reactivities of the anion precursors was available in the amount of TBP used in the selenium precursor. Early on, it was noted that sulfur binds strongly to TBP, so as to inhibit CdS nucleation and growth. Since in the synthesis of the alloyed nanocrystals the anion precursors must be mixed in advance of the reaction, excess TBP in the selenium precursor could react with sulfur, changing the reactivity of the sulfur. To explore the effects of TBP on alloy homogeneity, nanocrystals were synthesized with selenium precursor solutions of 2.5%, 3.0%, and 8.3% by volume of TBP. Small aliquots of the nanocrystal solution were removed from the reaction vessel periodically so that RBS could be used to monitor the changing composition of the nanocrystals during growth.

Figure 7 shows the composition of alloy nanocrystals with a precursor sulfur fraction of 0.4 as a function of growth time. The same trends were seen for all compositions. As seen previously, nanocrystals made with 2.5% TBP precursor were spherical and had a sulfur concentration that was nearly constant throughout their growth, an indication of homogeneous alloying. Nanocrystals produced using 3.0% TBP precursor remained spherical, but the sulfur concentration increased slightly with time, indicating a gradient structure. We explain the increasing sulfur concentration on the basis of the excess TBP. Prior to injection, the sulfur and selenium precursors were mixed, allowing any TBP not bound to selenium to bind to sulfur instead. When injected into the reaction vessel, the bound sulfur reacted much slower than selenium or unbound sulfur, causing initial sulfur concentrations that were lower than might be expected. Then, as available selenium depleted, sulfur was increasingly the only anion available for nanocrystal growth, causing the sulfur concentration on the exterior of the nanocrystal to increase, resulting in the observed gradient structure. The optical behavior of these nanocrystals also differed from those produced by the 2.5% precursor. Fluorescent quantum yields for the 3.0% TBP nanocrystals were higher, on the order of 0.30, as compared to yields of <0.01 for the 2.5% TBP

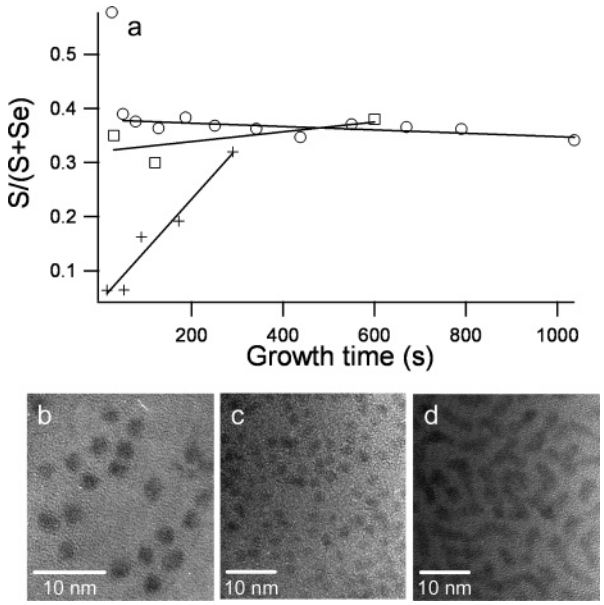

Figure 7. (top) Alloy composition as a function of growth time for $CdS_{0.4}Se_{0.6}$ grown using Se precursor solutions that were 2.5% (○), 3.0% (□), and 8.3% (+) TBP by volume. The 8.3% precursor shows a strong increase in sulfur with growth, indicating the formation of gradient alloys. The 3.0% precursor shows a slight increase in sulfur, and the 2.5% precursor a slight decrease. It is noted that the nanocrystals produced using the 2.5% TBP precursor were synthesized with the use of growth solution, unlike the 3.0% and 8.3% nanocrystals; the 2.5% nanocrystals are therefore much larger. (bottom) TEM images of nanocrystals synthesized using 2.5% (b), 3.0% (c), and 8.3% (d) TBP solutions. Lower amounts of TBP produce spherical nanocrystals, while higher amounts produce irregularly shaped nanorods.

nanocrystals and for pure CdS and CdSe. This is easily explained by the gradient structure; if the exterior had a higher concentration of sulfur, then electrons and holes in excited nanocrystals would be energetically confined to the center of the nanocrystal, enhancing fluorescence in the same manner as a core/shell structure. Moreover, a limited study on the band gaps of these nanocrystals yielded a bowing constant of 0.37 ± 0.23. Although this value agrees with the bowing constant of the 2.5% TBP nanocrystals within the uncertainty of the data, if the small increase is in fact real, then the 3.0% TBP nanocrystals behaved like homogeneous nanocrystals that were slightly smaller and slightly more selenium-rich, as could be expected from a gradient structure.

To explore further the effect of TBP on alloy growth, the TBP concentration was increased to 8.3%. With TBP in such excess, the gradient effect was greatly enhanced; the concentration of sulfur in the nanocrystals was initially almost nonexistent and increased dramatically with growth time. TEM images show that nanocrystals produced by this route were rodlike, suggesting that free TBP promotes growth along the *c* axis. Since they preferentially grew in a single direction and since previous work has shown that nanocrystals grow almost exclusively from the unpassivated anion-terminated face,[79,82] the gradient also likely propagated solely in this direction; certainly the quantum yield of these nanocrystals was no greater than the 3.0% TBP nanocrystals, indicating that the selenium-rich portion of these nanocrystals is no more shielded from the exterior than the 3.0% TBP nanocrystals. Although the 8.3% TBP nanocrystals were the wrong structure and composition for this study and were

(82) McBride, J. R.; Kippeny, T. C.; Pennycook, S. J.; Rosenthal, S. J. *Nano Lett.* **2004**, *4*, 1279−1283.

therefore quickly abandoned, they nonetheless remain an intriguing structure with potential applications in nanoelectronic devices. The one-dimensional gradient may generate gradient energy bands that could funnel charges unidirectionally; similar structures can be found in bulk semiconductor devices. Thus, simply by altering the amount of TBP in the reaction, it is possible to create homogeneous alloys, highly fluorescent gradient alloys, and unidirectionally gradient alloys.

Conclusions

We report for the first time the synthesis of homogeneously alloyed, zinc-blende CdS_xSe_{1-x} nanocrystals in all proportions. The band gap of these nanocrystals can be tuned by size or by composition, enabling the selection of more than one property (e.g., size and color) for specific applications. The dependence of the band gap on alloy composition is found to be slightly nonlinear, with a bowing constant of 0.29, in close agreement with bulk values; the bowing is not measurably size-dependent. In addition, the amount of TBP used in the reaction alters the morphology of the resultant nanocrystals, generating anything from homogeneous, spherical nanocrystals to one-dimensional, gradient nanorods, which may have applications in nanoelectronic devices.

Acknowledgment. The authors gratefully acknowledge Dr. Anthony Hmelo for training in the use of the RBS spectrometer and Dr. Charles Lukehart for training and use of the XRD spectrometer. L.A.W. was supported by a Stephen H. Cook fellowship. T.L.W. was supported by a National Science Foundation IGERT fellowship (DMR-0333392). Funding for this work was provided by the Department of Energy (DEFG0202ER45957) and the National Institutes of Health (RO1 EB003728).

JA063939E